Published in final edited form as:
Int J Biol Macromol. 2011 November 1; 49(4): 794–800. doi:10.1016/j.ijbiomac.2011.07.012.

Structural insight into the low affinity between *Thermotoga maritima* CheA and CheB compared to their *Escherichia coli* / *Salmonella typhimurium* counterparts

SangYoun Park[1,*] and **Brian R. Crane**[2]

SangYoun Park: psy@ssu.ac.kr; Brian R. Crane: bc69@cornell.edu

[1]School of Systems Biomedical Science, Soongsil University, Seoul, Korea

[2]Department of Chemistry and Chemical Biology, Cornell University, Ithaca, New York, USA

Abstract

CheA-mediated CheB phosphorylation and the subsequent CheB-mediated demethylation of the chemoreceptors are important steps required for the bacterial chemotactic adaptation response. Although *Escherichia coli* CheB has been reported to interact with CheA competitively against CheY, we have observed that *Thermotoga maritima* CheB has no detectable CheA-binding. By determining the CheY-like domain crystal structure of *T. maritima* CheB, and comparing against the *T. maritima* CheY and *Salmonella typhimurium* CheB structures, we propose that the two consecutive glutamates in the β4/α4 loop of *T. maritima* CheB that is absent in *T. maritima* CheY and in *E. coli* / *S. typhimurium* CheB may be one factor contributing to the low CheA affinity.

Keywords

Bacterial chemotaxis; CheB; CheA; *Thermotoga maritima*; Protein-protein interaction

1. Introduction

Bacterial chemotaxis is a signal transduction cascade that allows bacteria to swim towards a higher concentration of attractants (nutrient) and a lower concentration of repellents. In response to the extracellular chemicals sensed from the membrane-spanning chemoreceptor, bacteria such as *Escherichia coli* alternates between a counter-clockwise (CCW) and a clockwise (CW) rotations of the flagella to swim. The CCW rotation aligns the flagella with its filament handedness and results in formation of a multiple flagella bundle, which generates a forward thrust for smooth-swimming. However, the CW rotation forces the flagella bundle to fall apart and results in a tumbling motion necessary to randomly change

[*]To whom correspondence should be addressed: SangYoun Park, PhD, School of Systems Biomedical Science, College of Natural Sciences, Soongsil University, 511 Sangdo-Dong, Dongjak-Gu, Seoul 156-743, Korea, Phone: 82-2-820-0456, Fax: 82-2-824-4383, psy@ssu.ac.kr.

Accession Code: Worldwide Protein Data Bank coordinate for *T. maritima* $CheB_N$ has been deposited with an accession code **3T8Y**.

Supporting information
Supplementary materials including one figure (Fig. S1. Co-elution analysis of recombinant CheA and CheB mixtures from *E. coli* or *T. maritima* origin) are provided as part of this study.

the swimming orientation. The relative amount of time spent in the CCW vs. CW rotation (i.e. smooth-swim vs. tumble) determines the overall bacterial locomotion against the existing chemical stimuli [1–10].

Chemotaxis signaling begins in response to change in chemoreceptor's ligand occupancy, which affects the auto-kinase CheA activity to phosphorylate a histidine residue on its phosphotransfer domain. The phosphoryl group on the histidine is immediately transferred to an aspartate residue on the two response-regulator proteins, CheY and CheB which interact with CheA at the P2 domain [11]. Phospho-CheY detaches from CheA, and interacts with the switch protein FliM at the flagellar motor complex to change the flagellar rotation. Unlike CheY with only the response regulator domain, CheB consists of the N-terminus CheY-like response regulator domain ($CheB_N$) and the C-terminus catalytic methylesterase domain. CheA-mediated CheB phosphorylation at the $CheB_N$ domain detaches CheB from CheA, and concomitantly opens the methylesterase catalytic surface to the chemoreceptor substrate [12–15]. The catalytic domain of CheB counteracts the methyltransferase CheR at the methylation site of the chemoreceptor. CheB-mediated hydrolysis of the methyl glutamate residues results in the deactivation of the chemoreceptor and sets a new threshold compared to the previous concentration of the chemical ligand. This adaptive feedback mechanism allows the bacteria to swim up chemical gradients by preventing saturation.

E. coli and *Salmonella typhimurium* both from the Enterobacteriaceae family have been the paradigm organisms for studying chemotaxis. Despite a wide occurrence of chemotaxis signaling throughout Bacteria and Archaea, differences among species have been reported from comparisons of chemotaxis proteins over evolutionary distinct species [16]. For instance in *E. coli*, chemotactic signal provided by CheY-P is extinguished by the CheY-phosphatase CheZ, whereas in *Bacillus subtilis* or *Thermotoga maritima*, multiple proteins such as CheC, CheX, and FliY function as the CheY-phosphatase [17–23]. In general, *E. coli* and *B. subtilis* represent two different families of chemotactic bacteria to the latter of which *T. maritima* is more closely related [20].

An intriguing finding that distinguishes *E. coli* and *T. maritima* (or *B. subtilis*) chemotaxis is the different interaction modes of CheA and CheY [24–26]. Similar regions of CheY and CheA P2 domain form the binding interface in the two bacterial species, but the orientation of the two proteins differ by approximately ~90° rotation. Distinct sets of CheA P2 domain and CheY residues that mediate binding in the two cases have conservation and compensation patterns which allow the structure-based delineation of the chemotactic systems into two subfamilies. The subfamily represented by *E. coli* includes species from the Pseudomonadales and Enterobacteriales orders (both from the γ-Proteobacteria class), and from the Burkholderiales order (β-Proteobacteria class). The subfamily represented by *T. maritima* includes a broader range of species from the phylum Firmicutes, Thermotogae, Spirochaetes and also Euryarchaeota (Archaea Domain). This suggests that some aspects of chemotaxis signaling represented by *T. maritima* (or *B. subtilis*) may be applicable to a more general subset of prokaryotes.

Another example of differences between the *E. coli* and *T. maritima* systems from our previous study was that CheA and CheB interaction seen for *E. coli* proteins was not observed between the *T. maritima* counterparts [24]. In this study we attempt to probe the differences of CheA recognition by comparing the newly determined crystal structure of the *T. maritima* $CheB_N$ domain of 1.9 Å resolution to the previously reported structures of *S. typhimurium* $CheB_N$ [15] and *T. maritima* CheY.

2. Materials and methods

2.1 Protein preparation

The gene encoding the response regulator domain of CheB ($CheB_N$; *T. maritima* residues 1–144) was PCR-cloned into the vector pET28a (Novagen). The protein was expressed with His_6-tag in *E. coli* strain BL21 (DE3) (Stratagene) using kanamycin selection (25 μg/mL) and isolated on Nickel-NTA loaded columns; His_6-tag was removed by thrombin (Roche) cleavage. The protein was further purified using a Superdex 200 sizing column (GE Healthcare) in gel-filtration buffer (50 mM TRIS pH 7.5 and 150 mM NaCl), and was concentrated by centrifugation (Amicon Centriprep). Protein concentration (~50 mg/mL) was quantified by absorption at λ=280 nm and further confirmed by SDS-PAGE.

2.2 Crystallization

Initial conditions for growing the *T. maritima* $CheB_N$ crystals were found from commercial screening solutions (Hampton Research). Crystallization screenings were performed at 25 °C by using hanging drop vapour diffusion method in 24-well Linbro plates. Protein (~50 mg/mL) and well-solutions were mixed in 1:1 ratio of total 2 μL volumes. Initial crystals were screened with organic additives for improved diffraction. Final diffraction quality crystals of $CheB_N$ grew by vapour diffusion against a reservoir of 15–20 % (v/v) t-Butanol, 0.1 M MES pH 6.5 and 10% (v/v) MPD. For phase determination, lead-derivative crystals were grown in the same condition with the addition of 1 mM lead (II) acetate directly into the protein solution.

2.3 Diffraction data collection

Diffraction data with lead-derivative $CheB_N$ were collected under a 100 K nitrogen stream at a tuneable NSLS beamline (X25) on a CCD detector (ADSC Quantum Q315). Despite ~40% sequence identity between *T. maritima* $CheB_N$ and *T. maritima* CheY, or *S. typhimurium* $CheB_N$, the homologous structures failed as a molecular replacement model. Hence for direct phasing using multiple wavelength anomalous diffraction (MAD), data at three different wavelengths were collected for the lead-derivative $CheB_N$ (Table 1). The crystal belongs to the space group $P2_12_12_1$ and contains two molecules per asymmetric unit. Data were processed with DENZO and SCALEPACK [27].

2.4 Structure determination and refinement

The initial map of $CheB_N$ was generated by SOLVE [28] after locating the two lead sites found in the Patterson space. $CheB_N$ model was automatically built with ARP/wARP and SIDEgui [29] in the CCP4 suite [30]. The final model (two $CheB_N$ molecules in asymmetric unit, residues 4–137 and residues 3–140) was further refined in CNS (R-factor = 0.229, R_{free} = 0.245; R_{free} is the R-factor for 10% of randomly selected reflections excluded from the refinement.) (Table 2) [31]. Structural figures were rendered with PyMol [32].

3. Results

3.1 Structure of the *T. maritima* CheB response regulator domain ($CheB_N$)

Isothermal titration calorimetry (ITC) experiments have demonstrated that *E. coli* $CheB_N$ and CheY bind to CheA with similar affinity (K_D = ~μM) [11]. However, we have previously reported that the binding of *T. maritima* full-length CheB or $CheB_N$ to either *T. maritima* full-length CheA or CheA P2 domain was not observable within the detection limit of ITC (K_D > 1 mM) despite the observable interaction between *T. maritima* CheY and CheA (K_D = ~μM) [24]. As part of this study, we have confirmed our previous ITC results by performing protein mobility experiments with size-exclusion gel filtration

(Supplementary material). Although being less quantitative than ITC, we have verified that *T. maritima* CheB behaves differently compared to *E. coli* CheB in its ability to bind to CheA.

To gain molecular insight on the different $CheB_N$ and CheA interactions in *E. coli* and *T. maritima* proteins, we have determined the crystal structure of the *T. maritima* $CheB_N$ and compared it with the previously reported structure of *S. typhimurium* $CheB_N$ whose protein sequence is 95% identical to the *E. coli* $CheB_N$. *T. maritima* and *S. typhimurium* CheB share 41% sequence identity (61% sequence similarity) over the $CheB_N$ sequence (The two share 39% sequence identity over their entire CheB sequences including the catalytic domain.). The structure was determined at 1.9 Å resolution using lead-derivatized MAD-phasing. In the asymmetric unit of the $CheB_N$ crystal, there are two identical $CheB_N$ molecules (C_α RMSD=0.157 Å), each composed of 5 α-helices and 5 β-sheets typical to the response regulator fold. The alternating β-sheets, α-helices and the intervening loops are numbered sequentially from β1-α1 to β5-α5, with loops named according to flanking α-helix and β-sheet as in the previously reported CheY and CheB structures (Fig. 1). The *T. maritima* and *S. typhimurium* $CheB_N$ structures are highly similar with 122 out of 138 *T. maritima* $CheB_N$ residues superimposing to *S. typhimurium* $CheB_N$ (C_α RMSD=1.688 Å Fig. 2A). When the *T. maritima* $CheB_N$ and *T. maritima* CheY sequences are compared, the two also share 44% sequence identity (61% sequence similarity) and the two structures are highly similar as well, with 110 *T. maritima* $CheB_N$ residues closely superimposing to *T. maritima* CheY (C_α RMSD=1.203 Å, Fig.1 and 2B).

The most pronounced differences in both the sequences and the structures of *T. maritima* $CheB_N$ and *S. typhimurium* $CheB_N$ (or *T. maritima* CheY) are located at the β4/α4 loop, α4, β5/α5 loop, and α5 (Fig. 1). As seen in the structures of CheY and CheA P2 domain complexes from both *E. coli* and *T. maritima*, α4-β5-α5 surface of CheY mediates the CheA-binding (Fig. 1). This same interface in $CheB_N$ is also important in sequestering the CheB catalytic domain prior to CheA-mediated phosphorylation [15].

3.2 Structural comparison of *T. maritima* and *S. typhimurium* $CheB_N$

To help rationalize the low CheA-binding affinity between the *T. maritima* $CheB_N$ and CheA we have compared the two $CheB_N$ structures from *T. maritima* and *S. typhimurium* [15]. The differences in the two $CheB_N$ structures mostly reside at α4-β5-α5 which is the surface in the homologous CheY that is responsible for the CheA interaction (Fig. 1 and 2A). For instance, α5 of *T. maritima* $CheB_N$ with two more helical residues (116-Leu-Thr-117, Fig. 1) is distorted compared to that of *S. typhimurium* $CheB_N$ (Fig. 2A). The 15° kink in α5 is mediated by Pro123 (120-QVAPELL-126) which is not conserved in *S. typhimurium* $CheB_N$ (Fig. 2A). As a consequence, the β5/α5 loop significantly diverges in the two $CheB_N$ structures (Fig. 2A). However, since the shorther β5/α5 loop of both *S. typhimurium* (or *E. coli*) and *T. maritima* CheY do not directly participate in CheA-binding in either *E. coli* or *T. maritima* CheY:CheA interface [24–26], it is difficult to conclude whether these differences contribute to CheA-binding.

However, a more relevant difference in the two $CheB_N$s with respect to CheA-binding deduced from the comparison to the reported CheY:CheA interface is located on the face of α4 which forms the direct CheA-binding interface in CheY. The α4 of *T. maritima* $CheB_N$ is shorter by one turn at the N-terminus compared to the α4 of *S. typhimurium* $CheB_N$, and the "89-Glu-Glu-90" residues of *T. maritima* $CheB_N$ at the start of α4 form a loop instead of a turn of α-helix mediated by "87-Gly-Lys-88" in *S. typhimurium* $CheB_N$ (Fig. 3). Since the $CheB_N$-aligned residues of α4 in CheY which follow the "Glu-Glu" of $CheB_N$ directly participates in CheA-binding observed in the CheY:CheA interface, "Glu-Glu" mediated loop of *T. maritima* $CheB_N$ can obstruct a possible CheA interaction.

On comparing the sequences of CheBs from ~1000 prokaryotes, we find that the "Gly-Lys" sequence of the α4 in *S. typhimurium* CheB only occurs in the order of Enterobacteriales of the γ-Proteobacteria class, which includes the genus *Escherichia, Salmonella, Shigella, Yersinia, Cronobacter, Citrobacter* (some species have Gly-Gln), *Enterobacter, Edwardsiella, Dickeya, Erwinia* (some species have Gly-Gln) and *Serratia*. Among the BLAST searched prokaryotes, only *Geobacter uraniireducens* of the δ-proteobacteria class also contained "Gly-Lys" at this region. The equivalent residues aligned for "Gly-Lys" in species other than the Enterobacteriales were either two consecutive glutamates as for the case of *T. maritima,* or contained at least a glutamate or a glutamine (ER/QA/EK/KE/TE/QE/VE/KE/QQ/KQ/QN).

3.3 Structural comparison of the *T. maritima* $CheB_N$ and *T. maritima* CheY

Prominent structural differences between *T. maritima* $CheB_N$ and CheY lie in the regions neighboring the CheA-binding α4-β5-α5 interface. Residues comprising β5/α5 loop and α5 are ~10 residues longer in $CheB_N$ than in CheY. This results in a significantly longer β5/α5 loop and α5 (each by 5 residues) of $CheB_N$ when compared to CheY (Fig. 1 and 2B). The *trans* peptide bond conformation of $CheB_N$ Pro110 (107-ITKPHGS-113, Fig. 2B) allows the accommodation of the longer β5/α5 loop. This is contrary to the conserved Pro105 of CheY forming a *cis* conformation. However, since the regions of β5/α5 loop lie outside the previously characterized CheY:CheA interface, these residues are less likely to determine the specificity towards CheA. *T. maritima* CheY also displays one turn of a 3_{10}-helix (PEM, Fig 2B) prior to α3, which is absent in *E. coli* CheY. However, the remoteness of the 3_{10}-helix from the α4-β5-α5 interface rules against its contribution to CheA-binding.

Much more relevant structural difference of *T. maritima* CheY and $CheB_N$ regarding CheA-binding is observed again in the β4/α4 loop as seen in the comparison of *T. maritima* and *S. typhimurium* $CheB_N$. The insertion of the "Glu-Glu" motif in the β4/α4 loop for *T. maritima* $CheB_N$ where the equivalent residues are missing for CheY is positioned to obstruct CheA-binding (Fig. 2B and Fig. 3). To test whether single residue substitutions in the β4/α4 loop generate $CheB_N$ variants with enhanced CheA-binding similar to CheY, we made several single residue $CheB_N$ point-mutants (G91Q, A92Q, V121Q, E124R and Q131K) which are potentially important in mediating CheA contact based on the sequence alignment with *T. maritima* CheY (Fig. 1 and Fig. 4B). However, none of these mutants had enhanced affinity for CheA (Result not shown). Moreover, neither the β4/α4 loop "Glu89/Glu90" deletion nor "Glu-Glu" substitution to "Gly-Lys (E89G/E90K)" as found in *E. coli* CheB had any effect (Result not shown). Comparisons of the electrostatic chemical potential surface of *T. maritima* $CheB_N$ and CheY (Fig. 4) indicate that "Glu-Glu" motif is just one of the several charge distribution differences seen in the two cases, which help explain why enhanced CheY-like binding might not occur from a single residue change or a "Glu-Glu" motif deletion. Hence, we conclude that CheA-binding is likely from such combined effect of surfaces with "Glu-Glu" motif being one factor.

4. Discussion

In this study we have confirmed that *T. maritima* $CheB_N$ (and CheB) has substantially lower affinity for CheA when compared to either *T. maritima* CheY or *E. coli* counterparts. Since we do not know of any study reporting *T. maritima* $CheB_N$ as a functional substrate of *T. maritima* CheA, it still remains to be seen whether the CheA phosphotransfer rate to CheB reflects the low CheA-binding compared to CheY. However, the apparent low binding affinity (K_D > 1 mM) for *T. maritima* CheB and CheA doesn't necessarily mean that these two proteins have a low probability of interaction in the context of the signaling complexes inside the bacterial cell. For instance, some chemoreceptors of *E. coli* and *S. typhimurium* contain a conserved pentapeptide sequence (NWETF) that binds to CheR and CheB [33, 34].

Although NWETF sequence is not conserved in *T. maritima* chemoreceptors [35], there is a possibility that *T. maritima* CheB is tethered to chemoreceptors in close proximity to CheA, thereby increasing the effective local concentrations of the two proteins. Nevertheless, it is still unexplainable that *T. maritima* CheB would retain the CheY-like CheA interaction domain, $CheB_N$, but not interact with CheA.

One possibility is that the increased temperature favored by *T. maritima*, which has an optimal growth range of 80 – 90°C, may facilitate the interactions of the two proteins since the strength of hydrophobic or ion pair interactions generally increases with temperature. However, *T. maritima* CheA and CheY interaction investigated over 25 – 75°C indicated that K_D (or ΔG for binding interaction) maintained a similar value despite the temperature variation [24]. Although we cannot completely rule out the effect of temperature on *T. maritima* CheB to CheA-binding, we would still expect to see some interactions between the proteins at room temperature.

To gain molecular insight on *T. maritima* CheB with a low binding affinity to CheA, we have determined the crystal structure of *T. maritima* $CheB_N$ and compared it with the previously determined structures of *T. maritima* CheY and *S. typhimurium* $CheB_N$. Structural comparisons pointed out the two consecutive glutamates of β4/α4 loop in *T. maritima* $CheB_N$ not seen in *T. maritima* CheY or *S. typhimurium* $CheB_N$. Assuming that $CheB_N$ and CheA binding modes are analogous to those of CheY and CheA, which uses the α4-β5-α5 interface, this extended loop is expected to interfere with CheA-binding. However, simple "Glu-Glu" deletion or "Gly-Lys" substitution of *T. maritima* $CheB_N$ failed to enhance CheA-binding, which may infer multiple residues are involved in determining the global feature of the α4-β5-α5 interface allowing CheA interaction (Fig. 4).

It is important to note that "Glu-Glu" of β4/α4 loop in *T. maritima* $CheB_N$ also clashes with the C-terminus CheB methylesterase domain when superimposed to the full-length *S. typhimurium* CheB structure (Fig. 3D). The structure of *S. typhimurium* CheB demonstrates that the catalytic domain interacts with the $CheB_N$ domain using the same α4-β5-α5 surface responsible for CheA-binding, and phosphorylation of the $CheB_N$ destabilizes interaction with the catalytic domain to expose the methylesterase active site in a mechanism that parallels the release of CheY-P from CheA [15]. Hence, our *T. maritima* $CheB_N$ structure implies that the existence of "Glu-Glu" in β4/α4 loop may also prohibit $CheB_N$ interaction with the CheB catalytic domain which otherwise is observed for *S. typhimurium* CheB.

For bacteria orders other than the Enterobacteriales, the β4/α4 loop of CheB contains at least one glutamate or one glutamine residues for the *T. maritima* "Glu-Glu" motif. Since most of these species also contain Gln-to-Glu converting deamidases (eg. CheD), we have also tested whether CheR-mediated methylation at this β4/α4 loop might be a prerequisite for CheA interaction. Moreover, CheR-mediated methylation consensus sequence (Ala/Ser-sm-X-**Glx**-**Glu**-X-sm-Ala/Ser, methylation residues are in bold; sm indicates small residues which are either Ala, Gly, Ser or Thr) determined for various *T. maritima* chemoreceptor [36] matched the sequences neighboring the *T. maritima* CheB "Glu-Glu" motif (Ser-Leu-Thr-Glu-Glu-Gly-Ala-Ala) with Leu as the only exception [Of note, the methylation site of a *T. maritima* chemoreceptor TM1428 (Ala-Leu-Ser-**Gln**-**Gln**-Leu-Arg-Ser, methylation residues are in bold) also have Leu instead of the smaller consensus residue.]. However, contrary to our expectation CheB treated with purified CheR and S-adenosylmethionine [36] showed no evidence of glutamate to methyl glutamate modification (Results not shown). It seems that the agreement of the CheB "Glu-Glu" region with the chemoreceptor methylation consensus sequence is likely coincidental, especially since the structure of the chemoreceptor methylation region is completely α-helical, whereas the relevant CheB region is half loop and half helix. Hence, caution should be exercised in making predictions

based on just the protein sequences, and whenever possible the structural constraints must be considered.

The two complex structures of CheA and CheY from *E. coli* and from *T. maritima* have delineated two chemotaxis subfamilies, and the *E. coli* subfamily includes species from the Enterobacteriales, Pseudomonadales as well as the Burkholderiales orders (see introduction). The former two orders belong to the γ-Proteobacteria class and the latter to the β-Proteobacteria class, which are the two closest classes in the proteobacteria phylogenic tree. However, since the CheB "Gly-Lys" motif is only limited to the Enterobacteriales order of the γ-Proteobacteria class, we can conclude that Gly-Lys divergence of $CheB_N$ at the β4/α4 loop occurred more recent in evolution than the divergence of $CheB_N$ domains from CheY, and also more recent than the divergence of two CheY subfamilies.

Our hypothesis that "Glu-Glu" in β4/α4 loop of *T. maritima* $CheB_N$ acting as one factor contributing to the low CheA affinity is based on the assumption that CheY and CheB interacts with CheA using the same structural elements. However from the facts that $CheB_N$ is much more conserved among species compared to CheY (24–26), and that *E. coli* CheB exhibits CheA binding with similar affinity to that of CheY (11), it has been suggested that CheA binds to CheB using alternative binding strategy than for CheY (25). Hence, a complex crystal structure of *E. coli* $CheB_N$ and CheA (P2 domain), may allow us to better understand the apparent low CheA-binding for *T. maritima* $CheB_N$. Although we had aimed to crystallize the complex, to date this has proven unsuccessful.

Supplementary Material

Refer to Web version on PubMed Central for supplementary material.

Acknowledgments

This work was supported by a NIH grant GM066775 to B.R.C. We thank J. Y. Park for graphical assistance during figure preparation. Research carried out (in part) at the National Synchrotron Light Source, Brookhaven National Laboratory, which is supported by the U.S. Department of Energy, Division of Materials Sciences and Division of Chemical Sciences, under Contract No. DE-AC02-98CH10886.

References

1. Borkovich KA, Simon MI. The dynamics of protein phosphorylation in bacterial chemotaxis. Cell. 1990; 63:1339–1348. [PubMed: 2261645]
2. Parkinson JS, Kofoid EC. Communication modules in bacterial signaling proteins. Annu Rev Genet. 1992; 26:71–112. [PubMed: 1482126]
3. Appleby JL, Parkinson JS, Bourret RB. Signal transduction via the multistep phosphorelay: not necessarily a road less travelled. Cell. 1996; 86:845–848. [PubMed: 8808618]
4. Goudreau PN, Stock AM. Signal transduction in bacteria: molecular mechanisms of stimulus-response coupling. Curr Opin Microbiol. 1998; 1:160–169. [PubMed: 10066483]
5. Berg HC. The rotary motor of bacterial flagella. Annu Rev Biochem. 2003; 72:19–54. [PubMed: 12500982]
6. Kojima S, Blair DF. The bacterial flagellar motor: structure and function of a complex molecular machine. Int Rev Cytol. 2004; 233:93–134. [PubMed: 15037363]
7. Wadhams GH, Armitage JP. Making sense of it all: bacterial chemotaxis. Nat Rev Mol Cell Biol. 2004; 5:1024–1037. [PubMed: 15573139]
8. Sourjik V. Receptor clustering and signal processing in E. coli chemotaxis. Trends Microbiol. 2004; 12:569–576. [PubMed: 15539117]
9. Parkinson JS, Ames P, Studdert CA. Collaborative signaling by bacterial chemoreceptors. Curr Opin Microbiol. 2005; 8:116–121. [PubMed: 15802240]

10. Inouye, M.; Dutta, R. Histidine Kinases in Signal Transduction. Academic Press; San Diego: 2002.
11. Li J, Swanson RV, Simon MI, Weis RM. The response regulators CheB and CheY exhibit competitive bind to the kinase CheA. Biochemistry. 1995; 34:14626–14636. [PubMed: 7578071]
12. Lupas A, Stock J. Phosphorylation of an N-terminal regulatory domain activates the CheB methylesterase in bacterial chemotaxis. J Biol Chem. 1989; 264:17337–17342. [PubMed: 2677005]
13. Stewart RC. Activating and inhibitory mutations in the regulatory domain of CheB, the methylesterase in bacterial chemotaxis. J Biol Chem. 1993; 268:1921–1930. [PubMed: 8420965]
14. Anand GS, Goudreau PN, Stock AM. Activation of methylesterase CheB: Evidence of a dual role for the regulatory domain. Biochemistry. 1998; 37:14038–14047. [PubMed: 9760239]
15. Djordjevic S, Goudreau PN, Xu Q, Stock AM, West AH. Structural basis for methylesterase CheB regulation by a phosphorylation-activated domain. Proc Natl Acad Sci USA. 1998; 95:1381–1386. [PubMed: 9465023]
16. Armitage JP. Bacterial tactic responses. Adv Microb Physiol. 1999; 41:229–289. [PubMed: 10500847]
17. Fuhrer DK, Ordal GW. Bacillus subtilis CheN, a homo-log of CheA, the central regulator of chemotaxis in Escherichia coli. J Bacteriol. 1991; 173:7443–7448. [PubMed: 1938941]
18. Garrity LF, Ordal GW. Chemotaxis in Bacillus subtilis: how bacteria monitor environmental signals. Pharmacol Ther. 1995; 68:87–104. [PubMed: 8604438]
19. Garrity LF, Ordal GW. Activation of the CheA kinase by asparagine in Bacillus subtilis chemotaxis. Microbiology. 1997; 143:2945–2951. [PubMed: 12094812]
20. Nelson KE, Eisen JA, Fraser CM. Genome of Thermotoga maritima MSB8. Methods Enzymol. 2001; 330:169–180. [PubMed: 11210497]
21. Zimmer MA, Tiu J, Collins MA, Ordal GW. Selective methylation changes on the Bacillus subtilis chemotaxis receptor McpB promote adaptation. J Biol Chem. 2000; 275:24264–24272. [PubMed: 10825179]
22. Rosario MM, Kirby JR, Bochar DA, Ordal GW. Chemotactic methylation and behavior in Bacillus subtilis: role of two unique proteins, CheC and CheD. Biochemistry. 1995; 34:3823–3831. [PubMed: 7893679]
23. Saulmon MM, Karatan E, Ordal GW. Effect of loss of CheC and other adaptational proteins on chemotactic behavior in Bacillus subtilis. Microbiol. 2004; 150:581–589.
24. Park SY, Beel BD, Simon MI, Bilwes AM, Crane BR. In different organisms, the mode of interaction between two signaling proteins is not necessarily conserved. Proc Natl Acad Sci USA. 2004; 101:11646–11651. [PubMed: 15289606]
25. McEvoy MM, Hausrath AC, Randolph GB, Remington SJ, Dahlquist FW. Two binding modes reveal flexibility in kinase/response regulator interactions in the bacterial chemotaxis pathway. Proc Natl Acad Sci USA. 1998; 95:7333–7338. [PubMed: 9636149]
26. Welch M, Chinardet N, Mourey L, Birck C, Samama JP. Structure of the CheY-binding domain of histidine kinase CheA in complex with CheY. Nat Struct Biol. 1998; 5:25–29. [PubMed: 9437425]
27. Otwinowski Z, Minor W. Processing of X-ray diffraction data in oscillation mode. Methods Enzymol. 1997; 276:307–325.
28. Terwilliger TC, Berendzen J. Automated MAD and MIR structure solution. Acta Crystallographica. 1999; D55:849–861.
29. Perrakis A, Morris RM, Lamzin VS. Automated protein model building combined with iterative structure refinement. Nat Struct Biol. 1999; 6:458–463. [PubMed: 10331874]
30. CCP4 (Collaborative Computational Project, Number 4). CCP4 suite: programs for protein crystallography. Acta Crystallogr D Biol Crystallogr. 1994; 50:760–763. [PubMed: 15299374]
31. Brünger AT, Adams PD, Clore GM, DeLano WL, Gros P, Grosse-Kunstleve RW, Jiang JS, Kuszewski J, Nilges M, Pannu NS, Read RJ, Rice LM, Simonson T, Warren GL. Crystallography and NMR system: a new software suite for macromolecular structure determination. Acta Crystallogr D Biol Crystallogr. 1998; 54:905–921. [PubMed: 9757107]
32. DeLano, WL. The PyMOL Molecular Graphics System. DeLano Scientific; San Carlos, CA, USA: 2002. http://www.pymol.org

33. Lai RZ, Bormans AF, Draheim RR, Wright GA, Manson MD. The region preceding the C-terminal NWETF pentapeptide modulates baseline activity and aspartate inhibition of Escherichia coli Tar. Biochemistry. 2008; 47:13287–13295. [PubMed: 19053273]

34. Lai WC, Hazelbauer GL. Carboxyl-terminal extensions beyond the conserved pentapeptide reduce rates of chemoreceptor adaptational modification. J Bacteriol. 2005; 187:5115–5121. [PubMed: 16030204]

35. Perez E, Stock AM. Characterization of the Thermotoga maritima chemotaxis methylation system that lacks pentapeptide-dependent methyltransferase CheR:MCP tethering. Mol Microbiol. 2007; 63:363–378. [PubMed: 17163981]

36. Perez E, Zheng H, Stock AM. Identification of methylation sites in Thermotoga maritima chemotaxis receptors. J Bacteriol. 2006; 188:4093–4100. [PubMed: 16707700]

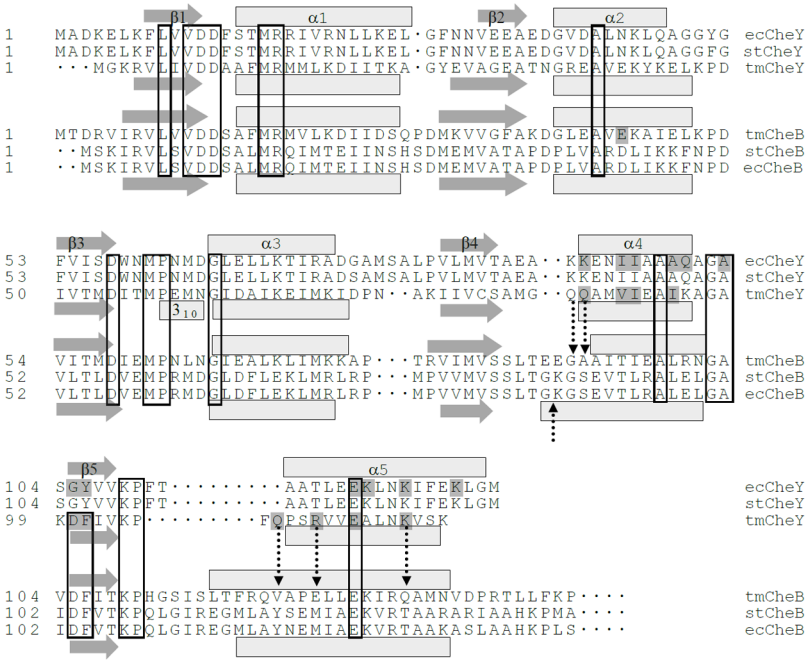

Fig. 1. Sequence alignment of $CheB_N$ and CheY from three organisms

$CheB_N$ and CheY sequences from *E. coli*, *S. typhimurium* and *T. maritima* were aligned by structure-based sequence alignment. Secondary structural elements are indicated as block rectangles (α-helix) and arrows (β-sheet) on top or below the corresponding amino acid residues. Residues conserved in all six sequences are boxed around the sequence. CheY residues from both *E. coli* and *T. maritima* shown to be critical for CheA-binding are highlighted in dark blocks. *T. maritima* $CheB_N$ residues selected for point-mutation to corresponding *T. maritima* CheY residues to test for CheA-binding are indicated with dotted arrows.

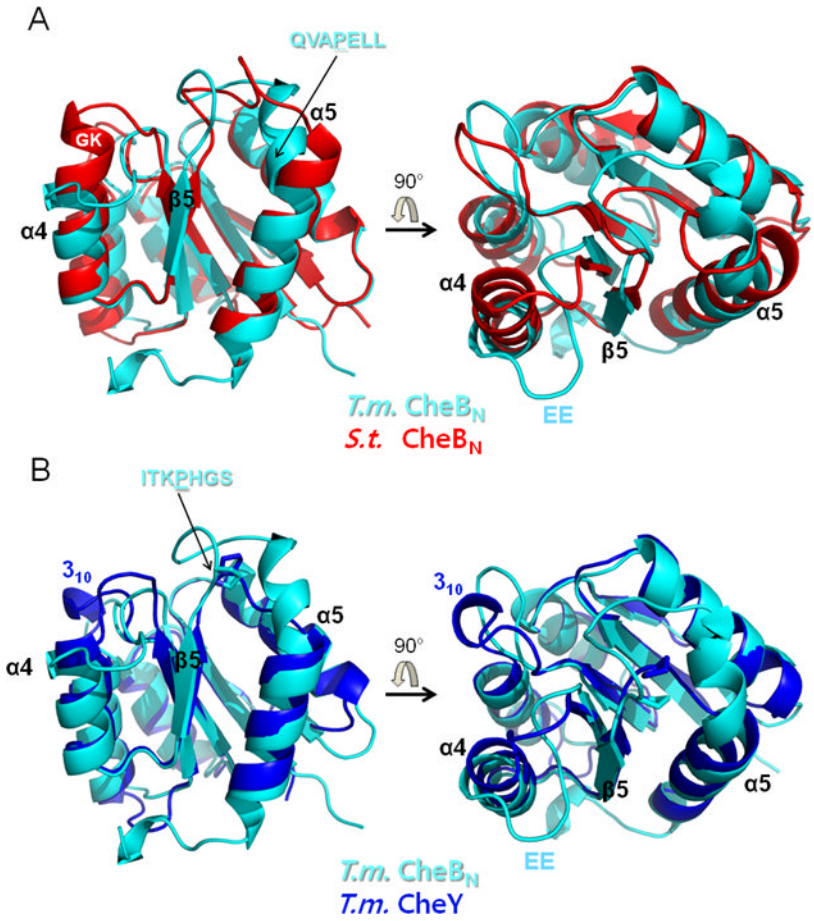

Fig. 2. Similarities and differences in the structures of *T. maritima* CheB$_N$, *S. typhimurium* CheB$_N$ and *T. maritima* CheY

(A) Superimposed structures of *T. maritima* CheB$_N$ and *S. typhimurium* CheB$_N$ are shown in two different orientations which are rotated 90° with respect to each other along the horizontal arrow. *T. maritima* CheB$_N$ has a longer α5 with Pro123 (QVAPELL) that kinks α5. The "Glu-Glu" of β4/α4 loop in *T. maritima* CheB$_N$ results in an extended loop whereas "Gly-Lys" at the equivalent region of *S. typhimurium* CheB$_N$ forms an extra turn of helix. The structure of *S. typhimurium* CheB$_N$ was rendered using PDB accession code, **1A2O**. (B) Superimposed structures of *T. maritima* CheB$_N$ and CheY are shown in two different orientations which are also rotated 90° with respect to each other along the horizontal arrow. Longer β5/α5 loop and α5 of *T. maritima* CheB$_N$ are spatially allowed by the *trans* peptide bond conformation of Pro110 (ITKPHGS) which is different from the *cis* form of the conserved CheY Pro105. For CheY, the "Glu-Glu" of CheB$_N$ is absent from the sequence, thus resulting in a shorter β4/α4 loop. The structure of *T. maritima* CheY was rendered using PDB accession code, **1U0S**. All figures were rendered with PyMol [32].

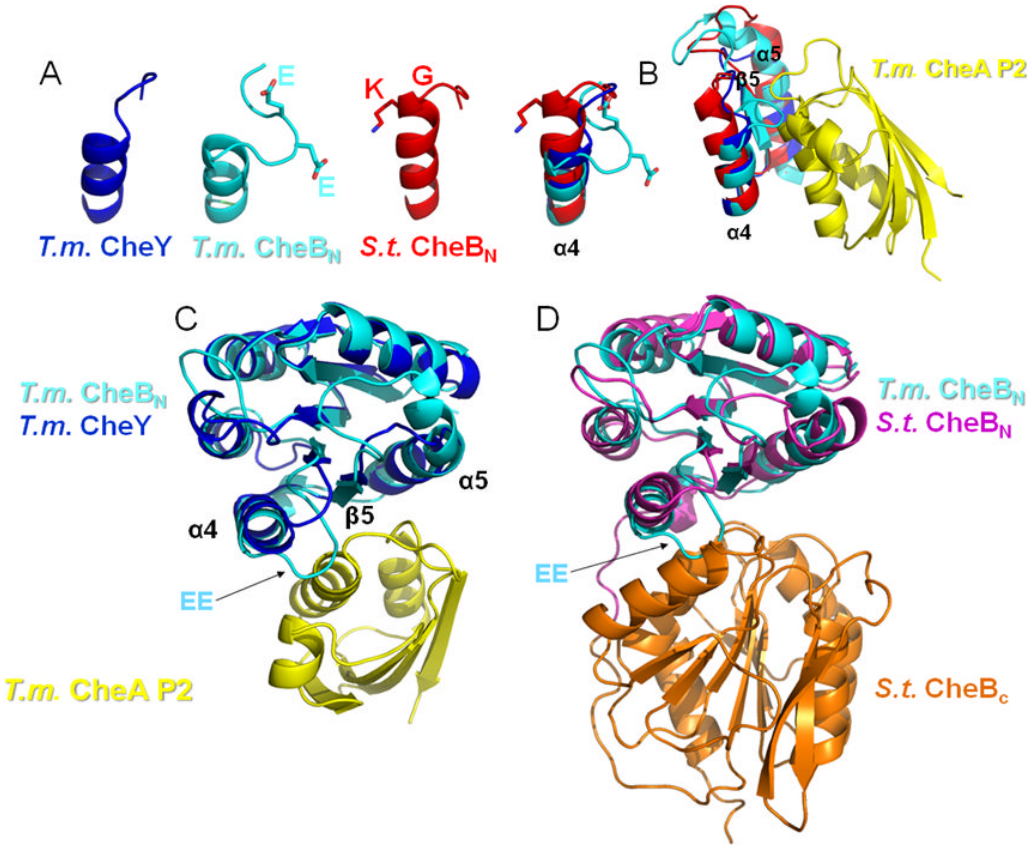

Fig. 3. Structural comparison of the β4/α4 loop and α4 in CheB and CheY proteins from *T. maritima* and *S. typhimurium*.

(A) The β4/α4 loop and α4 are compared for *T. maritima* CheB$_N$, CheY, and *S. typhimurium* CheB$_N$. (B) When the two CheB$_N$ structures are superimposed with *T. maritima* CheY:CheA P2 domain structure, only the "Glu-Glu" of the *T. maritima* CheB$_N$ β4/α4 loop clashes with the CheA P2 domain. The structure of *T. maritima* CheY:CheA P2 domain was rendered using PDB accession code, **1U0S**. (C) The "Glu-Glu" of the *T. maritima* CheB$_N$ β4/α4 loop may potentially block the proper CheB$_N$ interaction to CheA. (D) When *T. maritima* CheB$_N$ is superimposed with the *S. typhimurium* full-length CheB *via* CheB$_N$, the "Glu-Glu" clashes with the CheB catalytic domain (CheB$_C$). The structure of *S. typhimurium* CheB was rendered using PDB accession code, **1A2O**. All figures were rendered with PyMol [32].

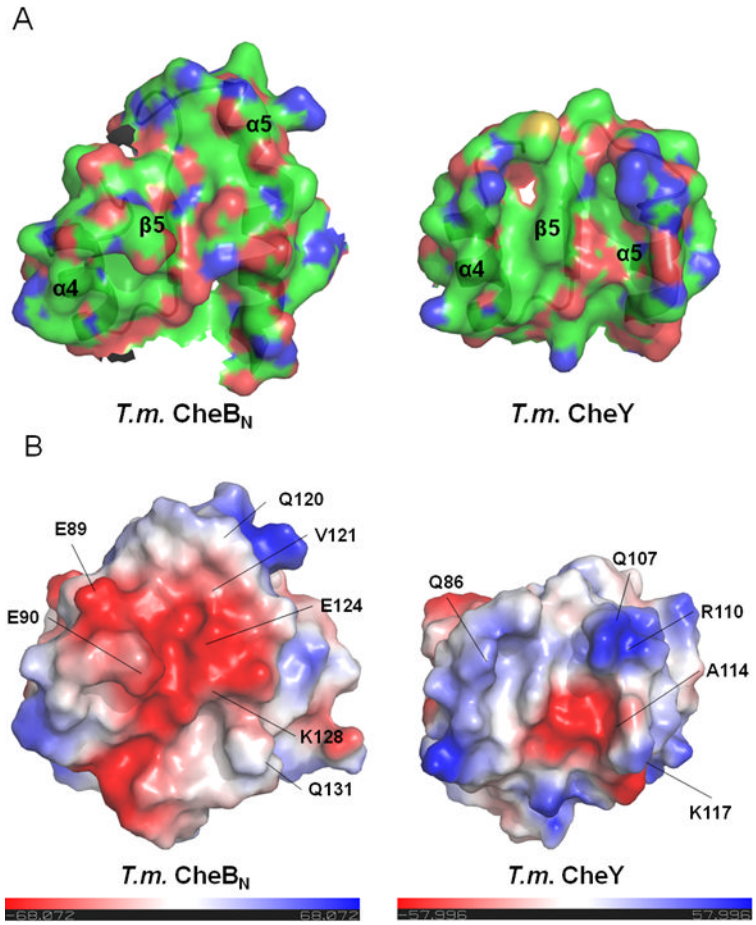

Fig. 4. Surface characteristics of *T. maritima* CheB$_N$ and CheY

(A) Chemical surface features of the α4-β5-α5 interface are highlighted using colors by residue type overlaid on top of the secondary structure elements. (B) Electrochemical potential features of the α4-β5-α5 interface are highlighted over the same orientation. Important CheY residues that mediate the CheA-binding, and the corresponding CheB$_N$ residues aligned to those are indicated. The structure of *T. maritima* CheY was rendered using PDB accession code, **1U0S**. All figures were rendered with PyMol [32].

Table 1

Data Collection and Phasing Statistics

	Pb-Peak	**Pb-Inflection**	**Pb-Remote**
Wavelength(Å)	0.949	0.950	0.918
Resolution(Å)	40-1.90	40-1.90	40-2.00
Highest Shell	(1.97-1.90)	(1.97-1.90)	(2.07-2.00)
Completeness (%)	97.8 (100.0)	97.7 (100.0)	98.4 (100.0)
R_{merge}[1]	0.052 (0.356)	0.052 (0.362)	0.053 (0.387)
I/σ(I)	34 (5)	34 (5)	32 (5)
Figure of Merit	0.67 (25-2.3 Å)		

[1] $R_{merge} = \Sigma\Sigma_j |I_j - \langle I \rangle| / \Sigma\Sigma_j I_j$

Table 2

Refinement Statistics

Space Group	$P2_12_12_1$ (a= 53.72 Å, b=53.68 Å, c=131.57 Å)
Resolution range (Å)	30-1.9
Unique Reflections (Test set)	54997(5445)
Wilson B ($Å^2$)	24.92
R-factor[1] (R_{free}[2])	0.229(0.245)
No. of Scatters (No. of residues)	4330(279)
No. of Pb molecules	2
No. of Water molecules	199
RMSD bonds (Å)	0.00782
RMSD angles(°)	1.327
Average B-factor (main chain) ($Å^2$)	29.18
Average B-factor (side chain) ($Å^2$)	32.5
Average B-factor (water) ($Å^2$)	43.65

[1] R-factor = $\Sigma(|F_{obs}|-|F_{calc}|)/\Sigma|F_{obs}|$

[2] R_{free} = R-factor for 10% of randomly selected reflections excluded from the refinement